Absorption resonances in Λ-type three-level system in cesium vapor cell with buffer gas

Jie Ma (马 杰), Yanting Zhao (赵延霆), Lirong Wang (汪丽蓉), Jianming Zhao (赵建明), Liantuan Xiao (肖连团), and Suotang Jia (贾锁堂)

State Key Laboratory of Quantum Optics and Quantum Optics Devices; College of Physics and Electronics Engineering, Shanxi University, Taiyuan 030006

Received June 16, 2005

We report experimentally the transformation from the electromagnetically induced transparency (EIT) resonance to a dispersion-like signal and eventually to a nearly symmetric absorption resonance as coupling detuning increases in Λ-type three-level system in the cesium vapor cell with buffer gas at room temperature. The observed absorption resonance occupies some remarkable properties of the strong amplitude and the narrow linewidth in comparison with the case without buffer gas. The relation between linewidth of the enhanced absorption resonance and buffer gas pressure is studied. With pressure increasing, linewidth of the absorption resonance becomes narrow. The sub-natural linewidth is observed in Doppler-broadened cesium vapor cell in our experiment. The experimental results are in qualitative agreement with the numerical simulations.

OCIS codes: 020.1670, 300.1030, 300.3700.

Quantum coherent effects attracted much attention and played a very important role in nonlinear and quantum optics in recent years. There are many effects, due to the atomic coherence, such as amplification without inversion (AWI)[1], coherent population trapping (CPT)[2], electromagnetically induced transparency (EIT)[3], electromagnetically induced absorption (EIA)[4] etc.. The atomic coherence also has been used in various applications, for instance enhancing refractive index or nonlinear susceptibility[5], the velocity selected coherent population trapping[6], slow group velocity[7,8], and information storage[9].

The characteristics of spectral width occurring due to these coherent effects are determined by the inverse lifetime of an atom in the coherent superposition of ground states, which is usually limited by the interaction time of an atom with the applied laser radiation in atomic cell[10]. For obtaining narrow resonances it is a common method to add buffer gas to atomic vapor. Using buffer gas allows atom to diffuse out of the interaction region slowly by velocity changing collisions and at the same time to preserve the atoms ground state coherence because of the extremely low spin-exchange cross section[11].

In this paper we experimentally demonstrate the transformation of the transmission peaks corresponding to EIT into absorption peaks for proper laser coupling detuning in a cesium vapor with buffer gas Ne at room temperature. And we note that amplitude of absorption with buffer gas is obviously enhanced compared with that without buffer gas under the same conditions, and the linewidth of enhanced absorption becomes narrow with increasing buffer gas pressure. In our experiment when the coupling detuning reaches about 1122 MHz (in comparison with the transition $6^2S_{1/2}F = 4 \rightarrow 6^2P_{3/2}F' = 4$), the sub-natural linewidth (about 2.6 MHz) absorption is observed in a cesium cell with 62 Torr of Ne, the numerical simulations are made based on the density matrix equations. The experimental results are qualitatively in agreement with the simulations.

The schematic diagram of experimental setup is shown in Fig. 1. Ti:sapphire laser (Coherent MBR 110) with output of 40 mW serves as the coupling laser. The extended cavity diode laser (New Focus 6000) is used for the probe laser. Both laser systems operate near the cesium D_2 transition (852 nm). The probe laser free-running linewidth is checked to be less than 500 kHz (< 50 ms). Optical isolators are used to avoid the optical feedback to keep laser stable operation. The saturated absorption spectrum is used for the frequency reference. The probe laser output is shaped to near circular beam by shaping prism pair. The coupling and probe beams co-propagate through the cesium vapor cell with buffer gas, and the linear polarizations are orthogonal using a $\lambda/2$ wave-plate for measuring the transmission. Two polarization beam splitter cubes placed near cell are used to overlap and separate the coupling and probe beams. In our experiment the 50-mm-long cesium vapor cells with

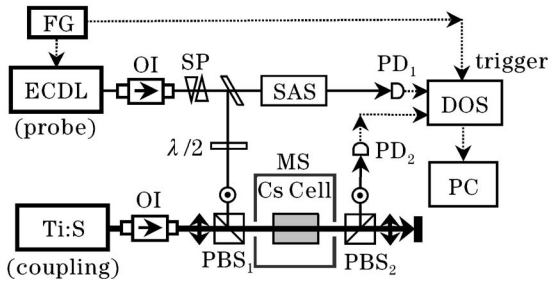

Fig. 1. Schematic diagram of the experimental setup. ECDL: external cavity diode laser; FG: function generator; OI: optical isolator; SP: shaping prism; SAS: saturated absorption spectrum; MS: magnetic shield; DOS: digital oscilloscope; PBS: polarization beam splitter; PD: photodiode; $\lambda/2$: half wave plate; PC: personal computer.

buffer gases of different pressures are placed in a magnetic shield tube to eliminate the influence of earth magnetic shield and other background magnetic fields and kept at room temperature. The diameter of the probe beam is 2 mm, which is smaller than that of the coupling laser ($\sim$ 4 mm) for a good overlapping. The power of the probe beam in front of the cell is typically 1 mW. After passing through the sample cell, the transmission of the probe laser beam was detected by a photodiode (Hamamatsu Si APD, S3884) and viewed and saved by a digital oscilloscope (Tektronix TDS1012) when the laser scans over the $6^2S_{1/2}F = 4 \rightarrow 6^2P_{3/2}F = 3$, 4, 5 transition, and then its output was transferred to a personal computer.

The relevant energy levels of cesium are schematically shown in Fig. 2. Considering the Λ-type three-level system formed by $|1\rangle$, $|2\rangle$, and $|3\rangle$, the common upper level $|3\rangle$ is the $6^2P_{3/2}F' = 4$ excited state, and the lower levels $|1\rangle$ and $|2\rangle$ are the $F = 3$ and $F = 4$ hyperfine states of the $6^2S_{1/2}$ ground state. The intensity of the probe beam is analyzed at the output of the cell as a function of the probe detuning δ. For a cesium cell without buffer gas, there are usually two different phenomena due to the coupling beam power. When coupling beam power is not too strong (for example, about 40 mW in Ref. [12]), the detected absorption reduction signal with a large coupling detuning is very weak. And sometimes it even cannot be found from the background[12]. The other case is that coupling beam power is strong enough (for example, 600 mW in Ref. [13]), the probe absorption can be observed with a large coupling detuning[13].

However, under the case of cells with a buffer gas, one can observe the different behaviors when coupling power is not too strong ($\sim$ 40 mW). For small coupling detuning, EIT resonance was still observed, as in the buffer-gas-free case. But as the detuning of coupling laser Δ increases, the EIT resonance becomes asymmetric, and gradually turns into a dispersion-like signal and eventually into a symmetric absorption resonance. Figure 3 shows the process of transformation in the cesium vapor cell with 20 Torr of Ne. In our experiment the similar transformations are also observed in cesium vapor cell with buffer gas in the presence of 1, 5, 10, 30, and 62 Torr of Ne. We find some important and valuable

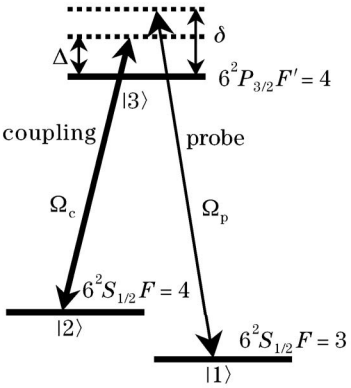

Fig. 2. Sketch of the relevant energy levels of cesium D_2 transition and the Λ-type three-level scheme. Δ is the detuning of the coupling laser, and δ is the detuning of the probe laser, which is scanned. Ω_c and Ω_p are the Rabi frequencies of the coupling and probe fields.

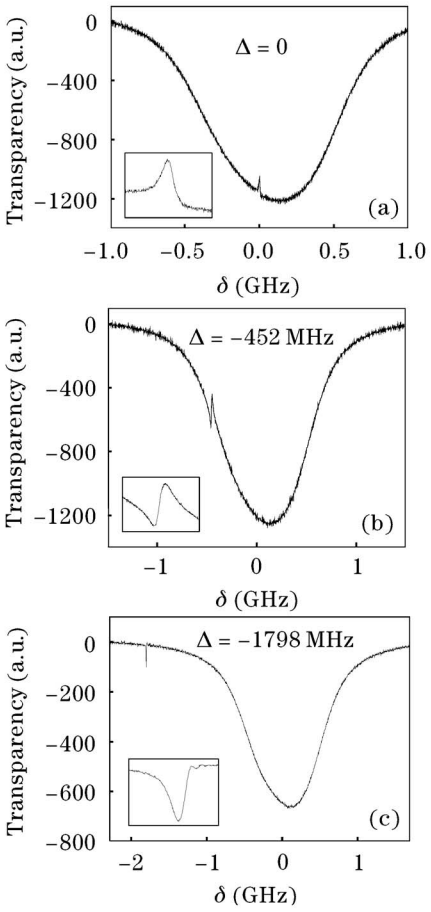

Fig. 3. Transmission of the probe field as a function of probe detuning δ for various coupling detuning Δ in cesium with 20 Torr of Ne. The insets enlarge the valuable regions.

properties about these absorption resonances.

First, we can easily note the amplitude of those absorption resonances in comparsion with the case without buffer gas. When the other conditions are the same, for example, with not strong coupling laser power, for large detuning and at room temperature, the amplitude of absorption peak with buffer gas is obviously larger than that without buffer gas (see Fig. 4). And the amplitude of the enhanced absorption peak observed for large

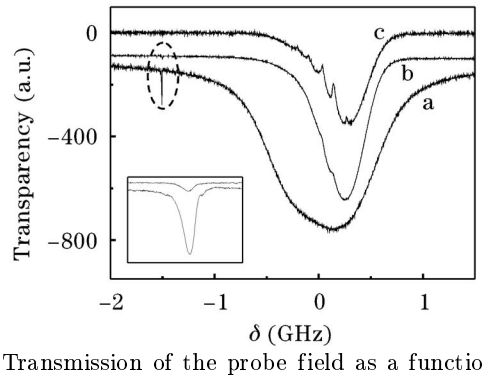

Fig. 4. Transmission of the probe field as a function of the probe detuning δ for coupling detuning $\Delta = -1480$ MHz in a cesium cell with 10 Torr of Ne (a) and without buffer gas (b). (c) is the sturation absorption spectrum of cesium D_2 line $6^2S_{1/2}F = 4 \rightarrow 6^2P_{3/2}F' = 3, 4, 5$. The inset enlarges the valuable region.

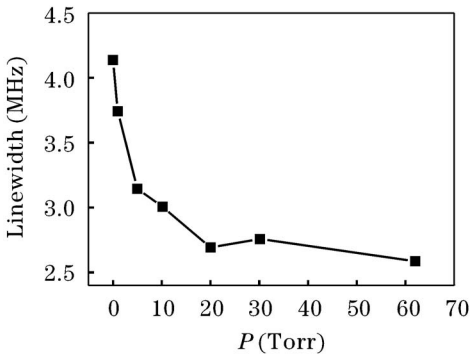

Fig. 5. Linewidth of the absorption resonance peaks with the same coupling detuning ($\Delta = 1122$ MHz) versus the pressure P of buffer gas.

detuning is comparable to, and sometimes larger than, the amplitude of the EIT peak at $\Delta = 0$.

Another important property of these absorption resonances is the narrowed linewidth. From Refs. [12] and [13] we know the sub-Doppler linewidth of the absorption peak for a large coupling detuning can be observed in cell without buffer gas. However, in our experiment the sub-nature linewidth of the absorption resonance is observed in Doppler-broadened cesium vapor cell with buffer gas. And the relation between the linewidth of absorption resonances and the different pressures of buffer gas is investigated as shown in Fig. 5. As pressure increases, linewidth of the absorption resonances becomes narrow, and eventually reaches to about 2.6 MHz under our experimental conditions, which is smaller than the cesium natural linewidth of 5.2 MHz. It is easy to understand the linewidth narrowing from the physical view. Because the collisions between cesium and buffer gas atoms or molecules do not destroy the quantum coherence of the internal states of the atoms, but effectively prolong the time they stay inside the laser beam(s), the signal linewidth becomes narrow[11].

In order to gain physical insight about this transformation from an EIT to a narrow enhanced absorption resonance, we have made numerical simulations based on the density matrix equations.

The three-level Λ-type scheme in Fig. 2 gives a simple and effective description of coherent effects in alkali-metal atoms[14]. The density matrix equations are

$$\dot{\rho}_{11} = i\Omega_{\rm p}^{*}\rho_{31} - i\Omega_{\rm p}\rho_{13} + \gamma_{\rm r}\rho_{33} - \gamma_{12}\rho_{11} + \gamma_{12}\rho_{22}, \quad (1)$$

$$\dot{\rho}_{22} = i\Omega_{\rm c}^{*}\rho_{32} - i\Omega_{\rm c}\rho_{23} + \gamma_{\rm r}\rho_{33} - \gamma_{12}\rho_{22} + \gamma_{12}\rho_{11}, \quad (2)$$

$$\dot{\rho}_{31} = i\Omega_{\rm p}(\rho_{11} - \rho_{33}) + i\Omega_{\rm c}\rho_{21} - (\gamma + i\delta)\rho_{31}, \quad (3)$$

$$\dot{\rho}_{23} = i\Omega_{\rm c}^{*}(\rho_{33} - \rho_{22}) - i\Omega_{\rm p}^{*}\rho_{21} - (\gamma + i\Delta)\rho_{23}, \quad (4)$$

$$\dot{\rho}_{21} = i\Omega_{\rm c}^{*}\rho_{31} - i\Omega_{\rm p}\rho_{23} - [\gamma_{12} + i(\delta - \Delta)]\rho_{21}, \quad (5)$$

where $\Omega_{\rm c}$ and $\Omega_{\rm p}$ are the Rabi frequencies of the coupling and probe fields; Δ and δ are the detunings of the coupling and probe lasers; γ is the polarization decay rate, $\gamma = \gamma_{\rm r} + \gamma_{\rm deph}$, $\gamma_{\rm r}$ is the radiative decay rate of the excited state and $\gamma_{\rm deph}$ is the dephasing rate of the optical transition due to non-radiative effects; γ_{12} is the lifetime of coherence between ground states $|1\rangle$ and $|2\rangle$, which is mainly determined by the diffusion time of atoms in the interaction region.

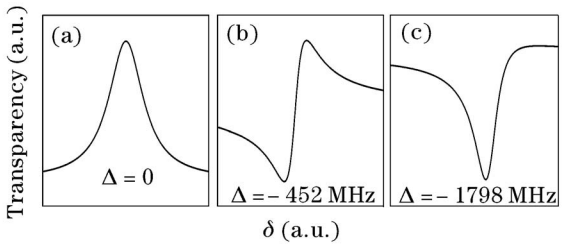

Fig. 6. Calculated probe field transmission spectra for the conditions corresponding to the experimental data in Fig. 3.

This absorption of the probe laser versus the probe detuning in Λ-type three-level system has been theoretically investigated by Mikhailov *et al.*[15]. Absorption coefficient α as a function of the probe detuning δ was given as[15]

$$\alpha = \frac{\kappa}{\gamma^2 + \Delta^2} \cdot \frac{\gamma\,|\Omega_{\rm c}|^2 + \gamma_{12}\Delta^2}{\gamma\,|\Omega_{\rm c}|^2 + 2\gamma_{12}\Delta^2} \cdot \frac{\gamma_{12}\,|\Omega_{\rm c}|^2 + \gamma(\delta - \Delta)^2}{(\delta - \Delta - \delta_0)^2 + \tilde{\gamma}^2}, \quad (6)$$

where $\kappa = 3N\gamma_{\rm r}\lambda^2/8\pi$, N is the cesium density, λ is the wavelength of the probe field, δ_0 is the ac Stark shift of the excited state, and $\tilde{\gamma}$ is the effective width of the probe transmission resonance.

The effect of the buffer gas is shown by both γ_{12} and $\gamma_{\rm deph}$ based on the atomic diffusion in the buffer gas. Figure 6 shows that the results of our simulations agree with the experimental results of Fig. 3. However, by carefully analyzing we can find that the results of numerical simulations provide only qualitative agreement with the experimental results. It is mainly due to ignoring some effects in the theoretical model, for example, Doppler background, the hyperfine structure of the excited state, and the Zeeman substructure.

We have experimentally investigated the transformation of resonances from an EIT peak to a dispersion-like signal and eventually to a nearly symmetric absorption resonance as coupling detuning increases in Λ-type three-level system in the cesium vapor cell with buffer gas at room temperature. We note some obvious differences between cells with and without buffer gas. When the coupling laser operates with a large detuning, the amplitude of the absorption peak is comparable to, and sometimes larger than, the amplitude of the EIT peak at zero detuning. As pressure increases, linewidth of the absorption resonances becomes narrow. The sub-natural linewidth is observed in Doppler-broadened cesium vapor cell under our experimental conditions. Narrow resonances with good signal-to-noise ratio are important for many applications. For example, narrow resonances are used for precision metrology and atomic clocks[15]. In the next work, we hope the narrow resonances with large amplitude can be used to get the better results in the experiment of four-wave maxing.

This work was supported by the National Natural Science Foundation of China (No. 10174047) and the Natural Science Foundation of Shanxi Province. J. Zhao is

the author to whom the correspondence should be addressed, her e-mail address is zhaojm@sxu.edu.cn.

References

1. S. E. Harris, Phys. Rev. Lett. **62,** 1033 (1989).
2. G. S. Agarwal, Phys. Rev. Lett. **71,** 1351 (1993).
3. K.-J. Boller, A. Imamoğlu, and S. E. Harris, Phys. Rev. Lett. **66,** 2593 (1991).
4. A. M. Akulshin, S. Barreiro, and A . Lezama, Phys. Rev. A **57,** 2996 (1998).
5. A. S. Zibrove, M. D. Lukin, L. Hollberg, D. E. Nikonov, M. O. Scully, H. G. Robinson, and V. L. Velichansky, Phys. Rev. Lett. **76,** 3935 (1996).
6. S. Kulin, B. Saubamea, E. Peik, J. Lawall, T. W. Hijmans, M. Leduc, and C. Cohen-Tannoudji, Phys. Rev. Lett. **78,** 4185 (1997).
7. L. V. Hau, S. E. Harris, Z. Dutton, and C. H. Behroozi, Nature **397,** 594 (1999).
8. D. Budker, D. F. Kimball, S. M. Rochester, and V. V. Yashchuk, Phys. Rev. Lett. **83,** 1767 (1999).
9. D. F. Phillips, A. Fleischhauer, A. Mair, R. L. Walsworth, and M. D. Lukin, Phys. Rev. Lett. **86,** 783 (2001).
10. E. Arimondo, Phys. Rev. A **54,** 2216 (1996).
11. M. Erhard and H. Helm, Phys. Rev. A **63,** 043813 (2001).
12. J. Wang, Y .Wang, S. Yan, T. Liu, and T. Zhang, Appl. Phys. B **78,** 217 (2004).
13. Y. Zhu and T. N. Wasserlauf, Phys. Rev. A **54,** 3653 (1996).
14. H. Lee, Y. Rostovtsev, C. J. Bednar, and A. Javan, Appl. Phys. B **76,** 33 (2003).
15. E. E. Mikhailov, I. Novikova, Y. V. Rostovtsev, and G. R. Welch, Phys. Rev. A **70,** 033806 (2004).